GEOPHYSICAL RESEARCH LETTERS, VOL. 37, L07804, doi:10.1029/2010GL042675, 2010



# Effects of spatial non-uniformity of streamer discharges on spectroscopic diagnostics of peak electric fields in transient luminous events

Sebastien Celestin[1] and Victor P. Pasko[1]

Received 26 January 2010; revised 25 February 2010; accepted 1 March 2010; published 2 April 2010.

[1] The electric fields associated with streamer discharges in transient luminous events (TLEs) have been recently measured by considering the ratios of spatially integrated radiation intensities of band systems with different energy excitation thresholds. Following recent work by Naidis (2009) we demonstrate that due to strong spatial variations of the electron density and electric field in streamer heads such measurements may lead to a significant underestimation of the peak values of electric fields. The modeling analysis of streamers as a function of altitude, applied reduced electric field, and streamer polarity indicate that the ratios based electric fields derived from spectrophotometric data need to be multiplied by a corrective factor >1.4 for positive streamers and >1.5 for negative streamers, to obtain the true peak values of electric fields. **Citation:** Celestin, S., and V. P. Pasko (2010), Effects of spatial non-uniformity of streamer discharges on spectroscopic diagnostics of peak electric fields in transient luminous events, *Geophys. Res. Lett.*, *37*, L07804, doi:10.1029/2010GL042675.

## 1. Introduction

[2] Spectroscopic diagnostics of lightning related TLEs occurring in the upper-atmosphere allow for obtaining information on the electric field associated with these events. Indeed, the ratio of volume emission rates corresponding to excited states with different energy excitation thresholds, such as the second positive system of $N_2$ ($2PN_2$) and the first negative system of $N_2^+$ ($1NN_2^+$), is a sensitive function of the electric field. The related diagnostic techniques have been extensively developed for laboratory discharges. For example, *Gallimberti et al.* [1974] have studied the average electric field in corona discharges in air at atmospheric pressure and *Kozlov et al.* [2001] have determined the spatio-temporal distribution of the electric field in a streamer propagating in a dielectric barrier discharge in air at atmospheric pressure. Essentially the same approaches have been used to utilize the data recorded by the ISUAL instrument on FORMOSAT-2 satellite for studies of sprites. *Kuo et al.* [2005] used five selected sprite events recorded by the ISUAL instrument to estimate the strength of the electric field to be ~2–3.7$E_k$, where $E_k$ is the breakdown field. *Liu et al.* [2006] compared streamer modeling results with the ISUAL measurements and concluded that in order to agree with observations during initial stage of sprite development the maximum field driving emissions of a sprite event must be $\gtrsim 3E_k$. *Adachi et al.* [2006] analyzed twenty sprite events captured by ISUAL and estimated that electric fields of the streamer region were ~1–2$E_k$. *Adachi et al.* [2008] have reported electric fields of the streamer region between ~0.8$E_k$ and ~3$E_k$. *Kuo et al.* [2009] studied gigantic jets and established that these discharges involve electric fields ~3.4–5.5$E_k$.

[3] In a streamer, the head is usually responsible for the most part of ionization and excitation of species, and therefore is responsible for the most part of emission. However, the spatial non-uniformity of streamer discharges is such that the maximum excitation rates are not exactly located at the maximum electric field [*Naidis*, 2009]. Recently, it has been emphasized that the evaluation of the electric field through the ratios of spatially integrated emissions would lead to substantial deviations from the peak electric field in the streamer head, and it has been suggested that a correction by a factor of ~1.5 should be applied to find true peak values of electric fields in streamers [*Naidis*, 2009]. The purpose of this work is to accurately quantify this factor for interpretation of spectrophotometric data related to TLEs.

## 2. Streamer Model

[4] We use the drift-diffusion equations coupled with Poisson's equation [*Bourdon et al.*, 2007, equations (26)–(29)]. In this study, we consider the streamer propagation as purely axisymmetric. The transport and source parameters are taken from [*Morrow and Lowke*, 1997]. The drift of charged species is solved using a flux-corrected transport (FCT) method [*Bourdon et al.*, 2007]. The photoionization is taken into account through the 3-Group $SP_3$ method derived by *Bourdon et al.* [2007] and *Liu et al.* [2007].

[5] The streamer is initiated by placing a Gaussian plasma cloud in a high field region (>$E_k$), created by a small conducting sphere with high potential. The conducting sphere is immersed in a weak homogeneous electric field (<$E_k$) in which the streamer is propagating. Following [*Liu and Pasko*, 2006], to preserve similar conditions at different altitudes, the size of the conducting sphere $R_s$, as well as the characteristic dimension of the initial Gaussian densities $\sigma$ are scaled by the ratio between the air density at the ground $N_0$ and at a given altitude $N$, such that: $R_s = 10^{-3}\ N_0/N$ m and $\sigma = 10^{-4}\ N_0/N$ m. The value of the ambient homogeneous electric field $E_{\mathrm{amb}}$ is scaled such that $E_{\mathrm{amb}} = E_0 N/N_0$, where $E_0$ is the reference field at the ground level. The maximum of the initial Gaussian densities is defined as $n_0 = 10^{18}\ N^2/N_0^2\ \mathrm{m}^{-3}$. The electric potential of the conducting sphere is adjusted with $E_0$ in order to keep constant the magnitude of the electric field in the vicinity of the sphere,

[1]CSSL, Pennsylvania State University, University Park, Pennsylvania, USA.


0094-8276/10/2010GL042675

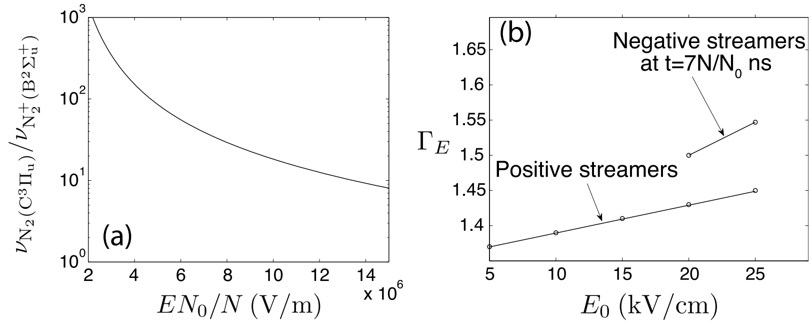


**Figure 1.** (a) Variation of the ratio $\nu_{N_2(C^3\Pi_u)}/\nu_{N_2^+(B^2\Sigma_u^+)}$ with respect to the reduced electric field. (b) Ratio $\Gamma_E$ between the actual peak electric field in the streamer head $E_h$ and field $E_m$ derived through integrated emissions of $N_2(C^3\Pi_u)$ and $N_2^+(B^2\Sigma_u^+)$.

similarly to the approach employed in [*Babaeva and Naidis*, 1997].

## 3. Spectroscopic Diagnostics

[6] During the streamer simulation we compute the evolution of excited species $N_2(C^3\Pi_u)$ and $N_2^+(B^2\Sigma_u^+)$ using the approach *Liu and Pasko* [2004, equation (6)]. The $N_2(C^3\Pi_u)$ and $N_2^+(B^2\Sigma_u^+)$ excited states are responsible for 2PN$_2$ and 1NN$_2^+$ emissions, respectively. Their lifetimes, quenching coefficients and excitation frequencies by electron impact are taken from [*Liu and Pasko*, 2004].

[7] The ratio between the excitation frequencies of $N_2(C^3\Pi_u)$ and $N_2^+(B^2\Sigma_u^+)$ is a sensitive function of the electric field. Having assumed steady state, from the knowledge of this ratio it is then possible to deduce the total electric field at a given location. The steady state assumption stipulates that the balance between creation of excited species by electron impacts and loss through quenching and radiative deexcitation is reached. Indeed, under the steady state assumption we get from [*Liu and Pasko*, 2004, equation (6)]:

$$\frac{I_{N_2(C^3\Pi_u)}}{I_{N_2^+(B^2\Sigma_u^+)}} = \frac{\nu_{N_2(C^3\Pi_u)}}{\nu_{N_2^+(B^2\Sigma_u^+)}} \frac{A_{N_2(C^3\Pi_u)}}{A_{N_2^+(B^2\Sigma_u^+)}} \frac{\tau_{N_2(C^3\Pi_u)}}{\tau_{N_2^+(B^2\Sigma_u^+)}} \quad (1)$$

where $I_k = n_k A_k$ is the volume radiative emission rate, $A_k$ is the Einstein coefficient of spontaneous emission, and $n_k$, $\tau_k$ and $\nu_k$ are, respectively, the number density, the characteristic lifetime, which accounts for the natural lifetime ($1/A_k$) and the quenching processes at a given altitude, and the frequency of creation by electron impact, of the exited species $k$. The dependence of $\frac{\nu_{N_2(C^3\Pi_u)}}{\nu_{N_2^+(B^2\Sigma_u^+)}}$ on the electric field is shown in Figure 1a.

[8] The quenching altitude of an excited species is defined as the altitude above which the loss of this excited species due to the quenching processes is exceeded by the loss due to spontaneous emissions. According to *Liu et al.* [2006], the quenching altitude of $N_2(C^3\Pi_u)$ is ~30 km, and the quenching altitude of $N_2^+(B^2\Sigma_u^+)$ is ~48 km. Note that the quenching altitude of the singlet states of nitrogen responsible for the photoionization is ~25 km.

[9] We have verified that the steady state assumption is fully justified for $N_2(C^3\Pi_u)$ and $N_2^+(B^2\Sigma_u^+)$ at altitudes above ~40 km ($N/N_0 \lesssim 3 \times 10^{-3}$). Whereas the characteristic lifetimes of the excited species $N_2(C^3\Pi_u)$ and $N_2^+(B^2\Sigma_u^+)$ do not significantly change with the altitude ($\tau_k \sim 1/A_k$) above 40 km, the characteristic spatial scales in the streamer vary as ~$1/N$. Below ~40 km, the characteristic time related to propagation of the highest field gradient in the streamer head becomes lower than the time required for the steady state to be attained (~$\tau_k$). Indeed, we have observed that the steady state of $N_2(C^3\Pi_u)$ and $N_2^+(B^2\Sigma_u^+)$ is not achieved below 40 km.

## 4. Results

[10] Figures 2a and 2b show cross-sectional views of the electron density and the electric field, respectively, for a pos-

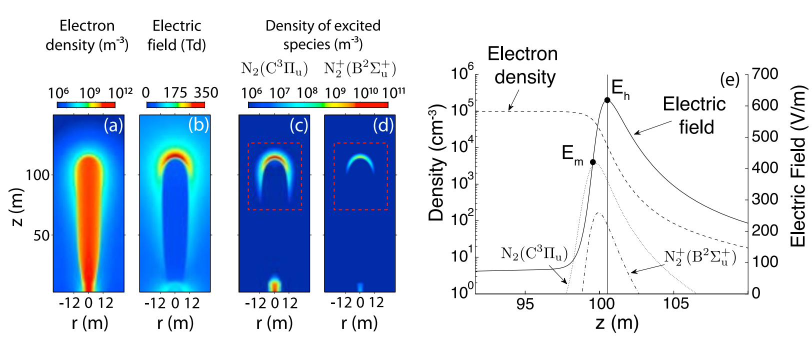


**Figure 2.** (a–d) Cross-sectional views of electron density, electric field, density of $N_2(C^3\Pi_u)$, and density of $N_2^+(B^2\Sigma_u^+)$, respectively, for a positive streamer simulated at 70 km altitude for $E_0$ = 15 kV/cm ($E_{amb} \simeq 10^{-3}$ kV/cm) at time $t$ = 214 $\mu$s. The dashed line represents the region of integration. (e) Distributions of densities of excited species ($N_2(C^3\Pi_u)$ and $N_2^+(B^2\Sigma_u^+)$), electric field and electron density on the axis of symmetry in the positive streamer head for a streamer propagating at 70 km altitude at $t$ = 258 $\mu$s for the case $E_0$ = 10 kV/cm ($E_{amb} \simeq 6.8 \times 10^{-4}$ kV/cm).

itive streamer simulated at 70 km altitude for $E_0$ = 15 kV/cm ($E_{amb} \simeq 10^{-3}$ kV/cm). Figures 2c and 2d show corresponding densities of $N_2(C^3\Pi_u)$ and $N_2^+(B^2\Sigma_u^+)$, respectively.

[11] The use of equation (1) to find the electric field at any point through the relation represented in Figure 1a is fully valid above 40 km, and therefore the use of the steady state assumption in the literature [e.g., *Kuo et al.*, 2005] is justified. However, as emphasized recently by *Naidis* [2009] and as depicted for a positive streamer in Figure 2e, the maximum of the electric field does not exactly correspond to the maximum of the density of excited states, and therefore to the maximum of light emission. Furthermore, the gradient of the field is extremely high in the region of the maximum intensities. For this reason, it has been recently suggested that computation of the peak electric field via spatially integrated intensities would lead to significant errors [*Naidis*, 2009]. In this context, the numerical simulation of streamers can quantitatively describe the corrections needed in processing experimental spectrophotometric data to measure peak electric fields in streamers using spatially integrated emissions. We have performed these simulations for both streamer polarities, at altitudes ranging from ground to 80 km, with a step of 10 km. For each altitude we studied $E_{amb}$ ranging from $5N/N_0$ kV/cm to 25 $N/N_0$ kV/cm, with a step of 5 $N/N_0$ kV/cm. The lower bound $E_0$ = 5 kV/cm is approximately equal to the stability field for positive streamers [e.g., *Babaeva and Naidis*, 1997]. The upper bound $E_0$ = 25 kV/cm has been recently found to be in very good agreement with observations of streamers in sprites [*Liu et al.*, 2009]. In the present work, stable propagation of negative streamers was obtained for $E_0$ > 15 kV/cm at ground pressure. Thus, the results reported in the present work on negative streamers correspond to $E_0$ = 20 and 25 kV/cm.

[12] From these simulations, we have spatially integrated the densities of $N_2(C^3\Pi_u)$ and $N_2^+(B^2\Sigma_u^+)$ over a region including the streamer head at given times (see dashed line in Figures 2c and 2d). From the ratio of these quantities and equation (1), assuming that the greatest contribution of the volume integral of the emissions are in the streamer head, and with the relation represented in Figure 1a, we estimate the electric field in the streamer head $E_m$ similarly to the electric fields derived using spectrophotometric data [e.g., *Morrill et al.*, 2002; *Kuo et al.*, 2005; *Adachi et al.*, 2006, 2008; *Kuo et al.*, 2009]. Then, we obtain the ratio $\Gamma_E = E_h/E_m$ between the actual peak field in the streamer simulations and the estimated peak field for a given $E_0$ and a given altitude. The ratio $\Gamma_E$ is plotted with respect to $E_0$ in Figure 1b and is valid for all altitudes >40 km.

[13] We have observed that the average effect due to the very small axial extension of the source terms of $N_2(C^3\Pi_u)$ and $N_2^+(B^2\Sigma_u^+)$ has a negligible contribution in $\Gamma_E$. However, because of the radial distribution of the streamer, the highest contribution to the total number of excited species comes from the regions away from the axis of symmetry. Additionally to the Naidis' effect, this results in reduction of $E_m$ by ~10% (increase of $\Gamma_E$ by ~25%). This geometric feature is automatically taken into account in the present study.

[14] For positive streamers, after a stage of initiation, the related ratio $\Gamma_E^+$ rapidly attains a constant value in time: $\Gamma_E^+ \simeq 1.4$. This value is very stable with respect to the altitude. In particular, for a given $E_0$, the ratio $\Gamma_E^+$ has been found to be constant above 40 km, since steady states of $N_2(C^3\Pi_u)$ and $N_2^+(B^2\Sigma_u^+)$ are attained and since the quenching altitude of excited levels of nitrogen responsible for photoionization is 25 km, i.e., streamers can be described through similarity laws [*Liu and Pasko*, 2006]. Even though the streamer is propagating in an external field above the stability field, in which case its radius increases in time, making its luminosity increase as well [*Liu et al.*, 2009], we have observed that $\Gamma_E^+$ is very stable. Moreover, $\Gamma_E^+$ slightly linearly depends $E_0$ (Figure 1b). We emphasize that the results presented in this article are related to the excited species $N_2(C^3\Pi_u)$ and $N_2^+(B^2\Sigma_u^+)$. The analysis conducted in [*Adachi et al.*, 2006, 2008] is primarily based on ratio of the spatially integrated excited states $N_2(C^3\Pi_u)$ and $N_2(B^3\Pi_g)$. Using those in our study leads to $\Gamma_E^+ \simeq 1.7$, possibly explaining the lower values of $E_m$ found by *Adachi et al.* [2006, 2008] compared to those found by *Kuo et al.* [2005].

[15] For negative streamers, the electric field in the streamer channel (this region is characterized by a high electron density behind the streamer head and is usually weakly luminous) has been observed to be high enough to produce a substantial emission of $2PN_2$ compared to the streamer head. Our analysis indicates that the integrated emission of $2PN_2$ cannot be considered as a signature of the high field in the negative streamer head, while in contrast the emission of $1NN_2^+$ is only significant in the streamer head. On the timescales of propagation studied in this work, the predominance of $2PN_2$ emissions coming from the streamer channel leads to a linear increase of $\Gamma_E^-$ in time, similarly to the luminous trail observed for positive streamers (see Discussion). However, in the case of negative streamers it is not possible to easily separate contributions of head and channel emissions. Figure 1b presents results of $\Gamma_E^-$ obtained at $t = 7N_0/N$ ns, after which $\Gamma_E^-$ increases linearly (see Discussion).

## 5. Discussion

[16] A significant density of the excited species has been observed in simulations of positive streamers close to the conducting sphere (see Figures 2c–2d), and this is especially true in high-field cases where this zone is expanding and becomes a *luminous trail* [*Liu et al.*, 2009; *Liu*, 2010]. Taking into account this region in the integration of density of excited species leads to even higher values of $\Gamma_E^+$ than the ones presented in Figure 1b. In fact, this involves an increase of $\Gamma_E^+$ with time, since the importance of this trail where the field is lower than $E_h$ becomes higher as this region expands. In Figure 1b, the integration of the densities of excited species has not been realized over the whole simulation domain, but over a volume including the emission of the streamer head, so that the information on $\Gamma_E^+$ that we present in Figure 1b is relevant to the streamer head dynamics. We emphasize that results on $\Gamma_E^+$ presented here can be considered as a lower limit for real sprite measurements. For the conditions of our model, integrating over the whole computational domain increased $\Gamma_E^+$ with a constant rate of $6.7N/N_0$ $\mu s^{-1}$ for $E_0$ = 25 kV/cm, leading in particular to an estimated ~8% increase in $\Gamma_E^+$ at 75 km and ~16% increase at 70 km on a typical time scale of ~500 $\mu$s propagation of positive streamers through this altitude range observed experimentally [*Stenbaek-Nielsen and McHarg*, 2008; *Liu et al.*, 2009]. This procedure may not be applicable for the long propagation times studied by *Morrill et al.* [2002].

[17] For negative streamers for $E_0$ = 20 and 25 kV/cm the rates of increase of $\Gamma_E^-$ were respectively: $10N/N_0$ $\mu s^{-1}$ and $30N/N_0$ $\mu s^{-1}$. Note that these results were obtained for $t \lesssim 20$ $N_0/N$ ns. We expect $\Gamma_E^-$ to become constant for very long streamers. Indeed, the total number of photons emitted by the streamer head per second varies like $r_s^3$, where $r_s$ is the streamer radius [*Liu et al.*, 2009]. If the field in the negative streamer channel does not vary in time the emission of the channel should vary like $r_s^2 \times L \sim r_s^3$ as well, since the streamer length $L$ is proportional to $r_s$ [*Liu and Pasko*, 2004; *Liu et al.*, 2009]. Therefore, the total emission of $2PN_2$ from the streamer body and the streamer head varies like $r_s^3$, similarly to the emission of $1NN_2^+$, although $1NN_2^+$ comes primarily from the streamer head.

[18] Concerning positive streamers propagating at altitudes lower than 40 km, although steady state of $N_2(C^3\Pi_u)$ and $N_2^+(B^2\Sigma_u^+)$ is not attained, the derivation of the electric field through integrated species can still be done. In fact, at a given time of the streamer propagation, if the streamer is stable enough (i.e., the velocity of the streamer and the total emission in volume can be considered as a time constant over the propagation time studied in the simulations of this work: ~$20N_0/N$ ns) only a delay of the radiative emissions is introduced. This delay can be observed in smoother and more spatially extended distribution of densities of excited species behind the positive streamer head. Carefully integrating the excited species over a region including the positive streamer head and the region behind the head where densities of excited species are still significant (for altitudes <40 km) allows for getting the information on the electric field responsible for their creation. The same analysis was not possible for negative streamers because of the non-negligible emission from the channel. The value of $\Gamma_E^+$ has been observed to vary less than 3% over the whole range of altitudes studied (0–80 km). The stability of $\Gamma_E^+$ with respect to altitude shows that non-similarity of streamers does not significantly affect $\Gamma_E^+$.

[19] We note that even for strong variations (×2.5) on the external electric field, $\Gamma_E^+$ varies only by approximately ~4%. *Liu et al.* [2009] have shown that $E_{amb} = 25N/N_0$ kV/cm matches with observational results for streamers in sprites. Assuming sprites mostly consist of downward propagating positive streamers, we emphasize that peak fields calculated in the literature from integrated spectrophotometric measurements [e.g., *Kuo et al.*, 2005; *Adachi et al.*, 2006, 2008] should be multiplied by $\Gamma_E^+ > 1.4$ (see Figure 1b and discussion in Section 4) to be consistent with the streamer theory of sprites.

[20] We also note that our work does not affect the previous conclusions of *Liu et al.* [2006]. Indeed, the comparisons between simulations and observations in [*Liu et al.*, 2006] were conducted using the integral number of photons emitted by the streamer, and were not based on peak fields in the streamer head.

## 6. Summary and Concluding Remarks

[21] In this article, we have simulated streamers propagating at altitudes from ground to 80 km. We have shown that there is a spatial shift between peak densities of $N_2(C^3\Pi_u)$ and $N_2^+(B^2\Sigma_u^+)$ and the peak electric field in streamer head. As suggested by *Naidis* [2009] for streamers at atmospheric pressure, we have observed that because of this shift $E_m$ significantly underestimates $E_h$ for both positive and negative streamers. However, the ratio $\Gamma_E^+ = E_h/E_m$ has been found to be very stable. For sprites studies we suggest to use $\Gamma_E^+ \simeq 1.41 \pm 0.04$ (see Figure 1b). The emission of the negative streamer channel has given rise to an increase of $\Gamma_E^-$ over the simulation timescales $t \lesssim 20$ $N_0/N$ ns and we observed that $\Gamma_E^- > 1.5$ after a propagation time of $7N_0/N$ ns. Since experimental studies conducted until now look at macroscopic structures, we have shown that those ratios are lower limits to be applied to existing spectrophotometric data on streamers in TLEs in order to deduce information about peak electric fields in these events. This study brings the values of electric field previously documented in the literature from observations [e.g., *Kuo et al.*, 2005; *Adachi et al.*, 2006] much closer to results of streamer simulations. Moreover, one can note that the value of $E_m = 5.5E_k$ documented in [*Kuo et al.*, 2009] for negative gigantic jet discharge would lead to the very high field $>1.5 \times 5.5E_k \simeq 8E_k$, approaching or exceeding magnitudes for which thermal electron runaway process becomes possible [e.g., *Moss et al.*, 2006; *Li et al.*, 2009; *Chanrion and Neubert*, 2010].

[22] **Acknowledgments.** This research was supported by the NSF grants ATM-0734083 and ATM-0741589 to Penn State University.

## References

Adachi, T., H. Fukunishi, Y. Takahashi, Y. Hiraki, R.-R. Hsu, H.-T. Su, A. B. Chen, S. B. Mende, H. U. Frey, and L. C. Lee (2006), Electric field transition between the diffuse and streamer regions of sprites estimated from ISUAL/array photometer measurements, *Geophys. Res. Lett.*, *33*, L17803, doi:10.1029/2006GL026495.

Adachi, T., et al. (2008), Electric fields and electron energies in sprites and temporal evolutions of lightning charge moment, *J. Phys. D Appl. Phys.*, *41*, 234010.

Babaeva, N., and G. Naidis (1997), Dynamics of positive and negative streamers in air in weak uniform electric fields, *IEEE Trans. Plasma Sci.*, *25*, 375.

Bourdon, A., V. P. Pasko, N. Y. Liu, S. Celestin, P. Ségur, and E. Marode (2007), Efficient models for photoionization produced by non-thermal gas discharges in air based on radiative transfer and the Helmholtz equations, *Plasma Sources Sci. Technol.*, *16*, 656.

Chanrion, O., and T. Neubert (2010), Production of runaway electrons by negative streamer discharges, *J. Geophys. Res.*, doi:10.1029/2009JA014774, in press.

Gallimberti, I., J. K. Hepworth, and R. C. Klewe (1974), Spectroscopic investigation of impulse corona discharges, *J. Phys. D Appl. Phys.*, *7*, 880.

Kozlov, K. V., H.-E. Wagner, R. Brandenburg, and P. Michel (2001), Spatio-temporally resolved spectroscopic diagnostics of the barrier discharge in air at atmospheric pressure, *J. Phys. D Appl. Phys.*, *34*, 3164.

Kuo, C.-L., R. R. Hsu, A. B. Chen, H. T. Su, L. C. Lee, S. B. Mende, H. U. Frey, H. Fukunishi, and Y. Takahashi (2005), Electric fields and electron energies inferred from the ISUAL recorded sprites, *Geophys. Res. Lett.*, *32*, L19103, doi:10.1029/2005GL023389.

Kuo, C.-L., et al. (2009), Discharge processes, electric field, and electron energy in ISUAL-recorded gigantic jets, *J. Geophys. Res.*, *114*, A04314, doi:10.1029/2008JA013791.

Li, C., U. Ebert, and W. Hundsdorfer (2009), 3D hybrid computations for streamer discharges and production of runaway electrons, *J. Phys. D Appl. Phys.*, *42*, 202003.

Liu, N. (2010), Model of sprite luminous trail caused by increasing streamer current, *Geophys. Res. Lett.*, *37*, L04102, doi:10.1029/2009GL042214.

Liu, N., and V. P. Pasko (2004), Effects of photoionization on propagation and branching of positive and negative streamers in sprites, *J. Geophys. Res.*, *109*, A04301, doi:10.1029/2003JA010064.

Liu, N., and V. P. Pasko (2006), Effects of photoionization on similarity properties of streamers at various pressures in air, *J. Phys. D Appl. Phys.*, *39*, 327.

Liu, N., et al. (2006), Comparison of results from sprite streamer modeling with spectrophotometric measurements by ISUAL instrument on FORMOSAT-2 satellite, *Geophys. Res. Lett.*, *33*, L01101, doi:10.1029/2005GL024243.

Liu, N., S. Celestin, A. Bourdon, V. P. Pasko, P. Ségur, and E. Marode (2007), Application of photoionization models based on radiative transfer and the Helmholtz equations to studies of streamers in weak electric fields, *Appl. Phys. Lett.*, *91*, 211501.

Liu, N. Y., V. P. Pasko, K. Adams, H. C. Stenbaek-Nielsen, and M. G. McHarg (2009), Comparison of acceleration, expansion, and brightness of sprite streamers obtained from modeling and high-speed video observations, *J. Geophys. Res.*, *114*, A00E03, doi:10.1029/2008JA013720.

Morrill, J., et al. (2002), Electron energy and electric field estimates in sprites derived from ionized and neutral $N_2$ emissions, *Geophys. Res. Lett.*, *29*(10), 1462, doi:10.1029/2001GL014018.

Morrow, R., and J. J. Lowke (1997), Streamer propagation in air, *J. Phys. D Appl. Phys.*, *30*, 614.

Moss, G. D., V. P. Pasko, N. Liu, and G. Veronis (2006), Monte Carlo model for analysis of thermal runaway electrons in streamer tips in transient luminous events and streamer zones of lightning leaders, *J. Geophys. Res.*, *111*, A02307, doi:10.1029/2005JA011350.

Naidis, G. V. (2009), Positive and negative streamers in air: Velocity-diameter relation, *Phys. Rev. E*, *79*, 057401.

Stenbaek-Nielsen, H. C., and M. G. McHarg (2008), High time-resolution sprite imaging: observations and implications, *J. Phys. D Appl. Phys.*, *41*, 234009.

S. Celestin and V. P. Pasko, CSSL, Pennsylvania State University, 227 EE East, University Park, PA 16802-2706, USA. (sebastien.celestin@psu.edu; vpasko@psu.edu)